

SUPERSONIC COMBUSTING JET EXPERIMENTS FOR CODE DEVELOPMENT AND VALIDATION^{*†‡}

A. D. Cutler and G. Magnotti
The George Washington University
Newport News, Virginia

D. P. Capriotti and C. T. Mills
NASA Langley Research Center
Hampton, Virginia

ABSTRACT

Computational fluid dynamics (CFD) methods based on the Reynolds averaged Navier-Stokes (RANS) equations are extensively employed in the design of hypersonic airbreathing engines. A fundamental weakness in these methods is the accurate mathematical modeling of turbulence and turbulence-combustion interactions. This paper is one of a companion pair of papers which describe the use of the combined dual pump CARS and newly developed interferometric Rayleigh scattering optical system to acquire time-accurate turbulence and mixing data with which to aid calibration and verification of the current turbulence models.

This test program consisted of a pilot laboratory-scale experiment used to develop the optical system and data acquisition techniques, and a significantly larger experiment to acquire the necessary turbulence data. The flow is an axially-symmetric, supersonic, combusting, free jet that provides good optical access, consisting of a central jet of hot "vitiated air" and a coflow jet of hydrogen or ethylene fuel. In this paper the development of both experiments is described. Facility and flow visualization data are presented for various types of flames, including the flames selected for detailed study with the CARS/Rayleigh optical techniques.

INTRODUCTION

BACKGROUND

Computational fluid dynamics (CFD) methods that employ the Reynolds-averaged Navier-Stokes (RANS) equations are widely used in the design and analysis of hypersonic airbreathing engine flow paths. These methods require models for various statistical properties of the turbulent fluctuations in flow variables. While models for the Reynolds shear stress are relatively well developed for low speed flows, these models are less well-developed for high speed, and new models are required for turbulent transport of chemical species and energy (Reynolds heat and mass flux), as well as for turbulence-chemistry interactions.¹

Turbulence models are mathematical approximations to very complex physical processes, and require experimental data for developing the form and for setting the constants.

* Approved for public release; distribution is unlimited.

† This effort was performed under sponsorship of the Defense Test Resource Management Center's (DTRMC) Test and Evaluation/Science and Technology (T&E/S&T) program, under the Hypersonic Test focus area, and by NASA's Fundamental Aeronautics Hypersonics Program. The GWU authors were supported through AEDC Contract FA9101-04-C-0013 and NASA Cooperative Agreement NNX07AC32A.

‡ Copyright © A. D. Cutler

Due to experimental difficulties, high quality data suitable for this development are lacking in supersonic combustion. Available data sets are limited to a subset of the important variables (temperature, composition, and velocity) and data sets that include accurate Reynolds stress, heat and mass fluxes do not exist. Even in subsonic reacting flows the simultaneous acquisition of temperature, composition, and velocity is experimentally very challenging. The situation is further complicated in supersonic flows where pressure becomes a variable, where experimental facilities become much more difficult and expensive to build and operate, and where often hostile environments are encountered (noise, heat, safety issues, etc.).

At NASA Langley Research Center, a sustained effort has been made to obtain experimental data for supersonic combustion model development. Data sets have been acquired in a H₂ fueled supersonic combustor using the coherent anti-Stokes Raman spectroscopy (CARS) technique² and the dual-pump CARS technique, originally developed by Robert Lucht and coworkers,^{3,4} and extended at Langley.^{5,6} The standard CARS technique is used to acquire temperature only whereas the dual-pump CARS technique is used to acquire both temperature and composition. Both mean flow and turbulence statistics (variances and covariances) were derived from the data, although the uncertainty in the latter was high due both to instrument error and to the small number of measurements with which to base the statistics on.

Other work includes Goynes, et al.⁷ who report measurements of mean streamwise velocity in a dual-mode scramjet using the particle-imaging velocimetry technique. International work in this area includes measurements in scramjet combustors conducted at ONERA (France) and DLR (Germany) using CARS⁸, and other non-intrusive techniques.

TEST MEDIA EFFECTS PROGRAM

Under sponsorship of the Office of the Secretary of Defense, and NASA's Fundamental Aeronautics Program, a program of experimental research has been undertaken to provide data suitable for model development and validation in both H₂ and hydrocarbon fueled supersonic combustors.^{9,10,11} Of particular interest is the development of models able to predict combustion and flame holding for scramjet/ramjet engines both in flight and tested in ground test facilities, and to enable ground test data to be extrapolated to flight. In these ground test facilities, the air entering the combustor is often replaced by "vitiating air", which is constituted to the same total sensible enthalpy as the air entering the engine in flight (in the frame of reference of the vehicle). Vitiating air is the product of combustion in air of either H₂ or a hydrocarbon that is enriched with O₂ to the same content (by mole or by mass) as standard air. This product approximately reproduces the pressure rise and thrust of the engine in air, but may not reproduce flame holding and other properties involving chemical kinetics in the engine flow field. The program includes instrumentation development, experimental facility and test technique development, data acquisition and analysis.

The previously developed dual-pump CARS system provides simultaneous instantaneous measurements of temperature and composition at a single point at a rate of 20 Hz. A new technique, interferometric Rayleigh scattering (IRS), has been developed to meet the need for simultaneous velocity measurements.^{12,13,14,15} This technique collects Rayleigh scattered light from one of the CARS laser beams and by spectral analysis to find Doppler shift, measures velocity in the same instant as the CARS measurement. Taken together, these measurements can be used to compute many of the statistical quantities of interest to the modeler, including terms relating to turbulent transport of species and energy.

Experiments have also been developed to provide suitable flows for study. An axisymmetric free jet was selected. This flow is geometrically simple, minimizing the number of spatial measurement points required to define the flow, and is accessible to optical instrumentation. There are several possible configurations: (i) a supersonic jet of fuel into stagnant air or low speed air coflow, (ii) a supersonic jet of fuel into supersonic air coflow, or (iii) a supersonic jet of air into low speed fuel coflow. Because of the requirement to study a high speed flow, one or both of the flows must be heated to ensure combustion. In some earlier work,

a laboratory burner was developed to provide a supersonic jet of combustion heated (vitiated) air coflow and a sonic jet of H₂ (or other fuel) at the axis - similar to (ii) above.¹⁶ Such a flow seemed ideal, but encountered many practical difficulties. The nozzle was not designed for uniform flow at the exit and consequently the jet contained a diamond shock system, forming Mach disks at the axis where the jet of H₂ was located. Mixing and combustion was dominated by these shocks. Additionally, the hardware was complex, and it was hard to maintain geometrical fidelity (the central jet of H₂ often was not on axis).

For the present research the flow is a heated sonic or supersonic center jet into an unheated low speed coflow. This flow was chosen since the apparatus to produce it is simpler than for a heated coflow. The center jet comprises the products of combustion of H₂, and can (at least in principle) be constituted to have excess unreacted H₂ or to have excess O₂ (i.e., be vitiated air). The coflow is low speed, unheated and can be either fuel or air. In either case the center jet is uniform and pressure matched to the atmosphere at the nozzle exit to avoid formation of shock waves in the external flow. Early computational studies focused on cases with a H₂ rich center jet, and designs were developed to ensure flame attachment at the nozzle exit.¹⁷ Subsequently, studies focused on cases in which the center jet was vitiated air and the coflow was a fuel, either H₂ or C₂H₄, or a mixture of these fuels. This change was, in part, because of an interest in studying combustion of a hydrocarbon fuel; if a hydrocarbon had been reacted to form the center jet flow, and the flow was fuel rich, then there would have been sooting which would have made the flow more complex than desired and interfered with the optical diagnostics. Operation with vitiated air is also the normal mode of operation of one of the facilities used in the experiments.

The main flow feature of interest, for the purposes of CFD model development, is the developing mixing layer between the center jet, the coflow and the surrounding ambient air, where combustion takes place. This layer thickness varies from near zero at the nozzle exit to roughly a nozzle exit diameter in thickness far downstream. In order to adequately resolve the turbulence in the layer, the measurement volume should probably be less than 0.1 × the thickness of the mixing layer. Turbulence fluctuations exist at much smaller scales than this, but the majority of the turbulence stress, and heat and mass flux are produced by the larger scales of the flow. The smaller scales are important in turbulent combustion since they are responsible for mixing of fuel and air to the molecular level, but cannot be resolved in a high speed (hence high Reynolds number) flow with the instrumentation available to us. Since the CARS measurement volume is approximately 1.5 mm long, this crude analysis suggests that the nozzle exit needs to be at least 15 mm diameter to resolve the turbulence far downstream, and much greater to resolve it near the nozzle exit.

Two different sizes of experimental hardware were developed. The first hardware was developed for the laboratory and is the largest that can safely be operated in that environment. This "laboratory burner" has a center jet nozzle exit diameter of 10 mm and is used to conduct preliminary flame studies and to verify the CARS-IRS techniques in the laboratory. The capstone experiments of this project, "the large-scale facility tests", were performed in NASA Langley's Direct Connect Supersonic Combustion Test Facility (DCSCTF),¹⁸ with a flow field that is essentially the same, but the nozzle exit diameter is 63.5 mm. The present paper briefly describes the laboratory burner and some results in that burner, but is focused on the design, facility measurements and flame visualization studies of the large scale tests. A complementary paper describes the CARS-IRS measurements in this facility.¹⁹

LABORATORY EXPERIMENT

Figure 1a shows the laboratory-scale burner, sectioned along the axis, with bolts, gas supply lines, spark plug and other fittings not shown. It consists of a water-cooled combustion chamber, an annulus and a nozzle. The nozzle, with 10 mm exit diameter, is interchangeable; convergent ($M \leq 1$), or supersonic convergent-divergent ($M = 1.6$ and $M = 2$), designed using the method of characteristics. An annular coflow nozzle is formed between the nozzle and the annulus. The coflow nozzle is convergent with exit width (in the radial direction) of 1 mm. The

annular base at the exit, between the central jet and coflow, is normal to the axis and 3 mm wide. Reactants at ambient temperature are delivered to the burner by the “injector”, a central tube through which gaseous fuel flows, and a concentric passage through which a mixture of O_2 (or sometimes N_2) with air flows. Various combinations of H_2 or C_2H_4 fuel, air, and O_2 are reacted in the combustion chamber to provide hot products at various temperatures and compositions (dependent on flow rates). The coflow may be of unheated fuel (H_2 or C_2H_4) or air. The resulting coaxial jet flow will mix and may react. If reaction does take place, then the flame may be held at the burner or stand off from it, depending on temperature and Mach number. Figure 1b is an image of the burner near the nozzle exit during operation showing a Mach 2 jet of vitiated air (air coflow, so no flame) and the laser beams of the CARS-Rayleigh system.

Reference 20 provides a detailed description and analysis of this burner, and visualization studies of the various flames. *Edge attached flames* were the result in cases with excess O_2 in the hot center jet (vitiated air) and H_2 coflow: these flames started at the interface between the ambient air and the H_2 coflow very close to the nozzle exit, and extended downstream. Flames detached from the nozzle exit if the centerjet Mach number was raised from 1.6 to 2. *Base attached flames* were the result in cases with excess H_2 in the center jet and air coflow: these flames started in the recirculating flow region at the nozzle base (i.e., at the interface between the coflow and the centerjet). Flames detached from the nozzle exit if the centerjet enthalpy was reduced below a certain threshold. Weak detached flames or no flames were the result in cases with vitiated air center jet and C_2H_4 coflow. Several of these flames will be discussed in section “Flame Visualizations” below.

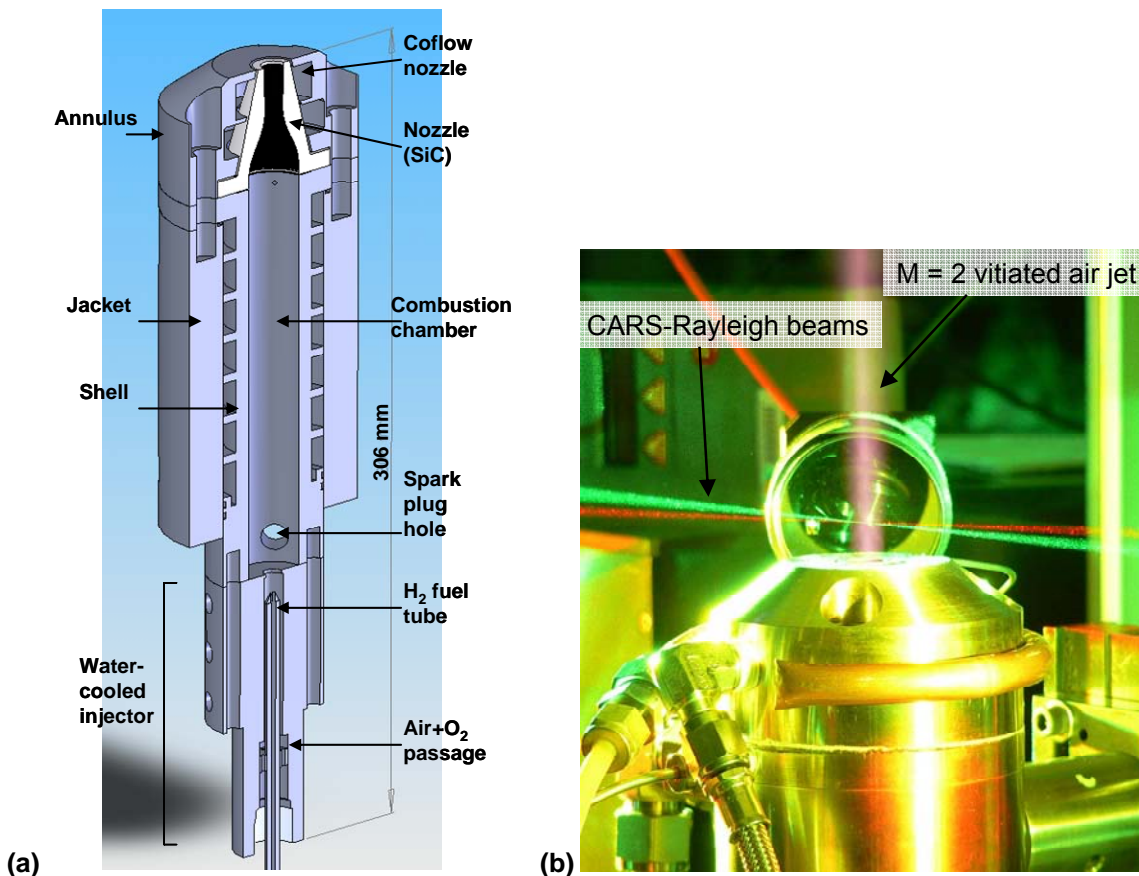


Figure 1. Laboratory scale burner: (a) vertical section view, (b) burner in operation showing laser beams (but no coflow flame).

LARGE SCALE FACILITY TESTS

NOZZLE AND FACILITY DESCRIPTIONS, INSTRUMENTATION

The nozzle for the large scale tests, which is axisymmetric except for bolts, instrumentation, etc., is illustrated in Figure 2. It consists of a water-cooled nickel mating flange, a water-cooled copper nozzle block, and a stainless steel cone. The heated center flow nozzle is formed within the copper block, and its contour was designed by the method of characteristics to provide a uniform Mach 1.6 flow at the exit, at the nominal test point. A coflow nozzle is formed by the space between the copper block and the steel cone. A sintered mesh porous plate is trapped between the cone and the block, forming the coflow plenum. The coflow gas (typically H_2 and/or C_2H_4) is supplied, unheated, to the coflow plenum; the gas passes through the porous plate, which distributes the flow uniformly around the circumference, and is accelerated in the nozzle. Mach number at the coflow nozzle exit is low, approximately 0.07, and the pressure in the coflow plenum (upstream of the porous plate) is approximately 650 kPa for the nominal test case studied with the CARS-IRS system (B.b in Table 2). The nozzle is instrumented with three spring-loaded thermocouples at the bottom of 6.35 mm diameter blind holes (from the outside) in the copper block. The bottom of these holes is located such that the thermocouple approximately measures the unperturbed nozzle surface temperature.² A fourth thermocouple is attached with ceramic glue to the base of the nozzle – the base is defined as the forward facing exterior surface between the center jet and coflow nozzle exits. A pressure tap is located in the nozzle ahead of the contraction.

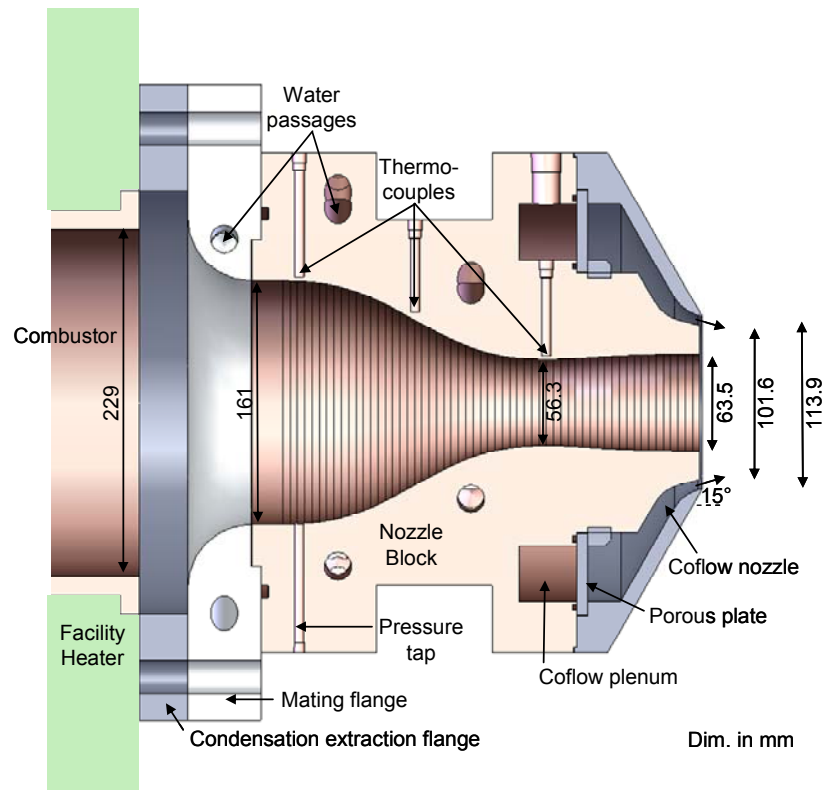


Figure 2. Horizontal section of large scale nozzle.

The nozzle is attached to the vitiated air heater of the Direct Connect Supersonic Combustion Test Facility. The heater provides the products of combustion of H_2 , O_2 and air to the nozzle. The combustion chamber of the heater is 229 mm internal diameter and

approximately 1.32 m long. At the upstream end, 12 injectors are distributed on a 127 mm diameter. Air and O₂ are premixed upstream and are made to enter the combustion chamber around the outside of each injector, while H₂ is made to enter through the center of each injector. The minimum flow area at each injector is 101 mm² for the air-O₂ mixture and is 1.37 mm² for the H₂.

Mass flow rates are measured with an uncertainty of ±3% using standard ASME, sharp-edged orifice plates, pressures are measured with an uncertainty of ±1% using strain gauge type pressure transducers, and temperatures are measured with an uncertainty of ±2 K or ±0.75% (whichever is greater) using type K thermocouples.

In addition to facility instrumentation, the free jet flow near the nozzle exit is monitored with an infrared light (IR) digital video camera, FLIR Model SC4000-MWIR, with sensitivity in the 3-5 μm range and electronic shutter exposure time set nominally to 12 μs. Video is also acquired in some runs with commercial grade visible light video cameras, which had a relatively long image integration time (1/30 s). Additionally, for certain cases the flow was extensively probed with the dual-pump CARS-interferometric Rayleigh scattering (CARS-IRS) optical system (these results have been reported separately).¹⁹ The nozzle installed in the facility is shown in Figure 3. Inset in this figure is an IR image of a case in which there is combustion of H₂ coflow. The flow is from left to right in this image as with all flame images, while the color is false (there is no spectral content in the image), and the brightness is in proportion to temperature. The brightness scale generally differs from one IR image to the next, so comparisons of brightness between images should not be made. Also, a few of the elements of the optical system may be seen in the picture.

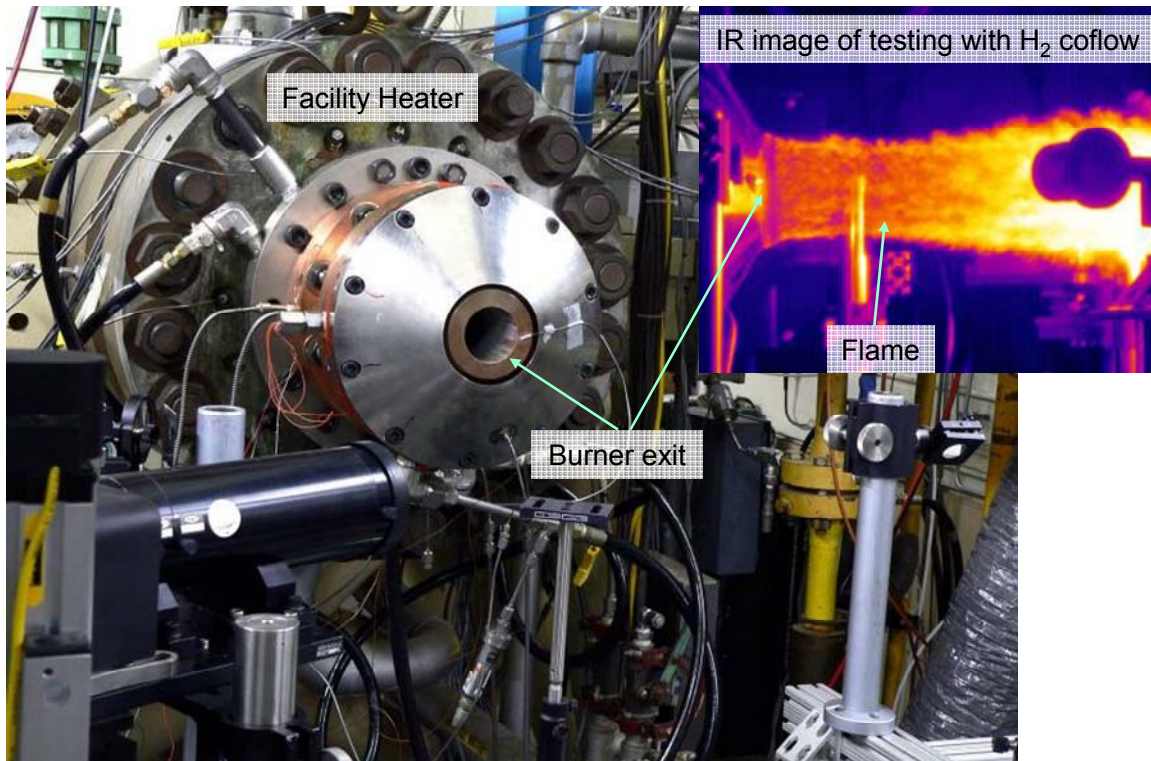


Figure 3. Image of nozzle installed in LaRC's Direct Connect Supersonic Combustion Test Facility; inset is IR image of flame.

TEST CONDITIONS, NOZZLE WALL TEMPERATURES

Test cases were for vitiated air in the center jet and either no coflow, or a coflow of a fuel. In principle, the facility could be operated to provide excess H_2 in the center jet, as in the laboratory. However, under normal operation the facility provides vitiated air: operation with excess H_2 would have been a new mode of operation requiring minor modifications to the combustor and testing to verify. Additionally, the rates of H_2 flow were high, raising safety concerns. Time constraints did not allow for these issues to be addressed, and this mode was not attempted.

Tests were conducted over a range of test gas temperatures, at enthalpy Mach numbers (M_h) from 5 to 7. (The enthalpy Mach number is the Mach number of flight for which the air in the reference frame of the vehicle has the same sensible total enthalpy as the test gas.) Facility flow rates were set to provide vitiated air with nominally the same mass fraction of unreacted O_2 in the products as is contained in air (23%). Facility flow rates for nominal conditions, as well as computations of the total pressure and temperature in the combustion chamber are provided in Table 1. Computations assume quasi-1D flow and that the heat loss from the combustion products to the facility (structure and cooling water) is 20% of the sensible enthalpy of the products, referenced to the reactant inflow temperature.² Flow rates of coflow are expressed in terms of an overall equivalence ratio between the coflow and the center jet ϕ ; an equivalence ratio of one implies that the unreacted fuel in one flow and the unreacted O_2 in the other could react completely to form H_2O (and CO_2) products.

M_h	Nominal condition		Flow rate (kg/s)		
	p_t (kPa)	T_t (K)	air	H_2	O_2
5	424	1163	1.038	0.0128	0.1358
5.5	419	1327	0.920	0.0144	0.1535
6	414	1504	0.816	0.0161	0.1712
7	405	1842	0.644	0.0195	0.2070

Table 1. DCSCTF flow rates at nominal operating conditions.

Nozzle wall temperatures at enthalpy Mach numbers from 5 to 7, both with and without coflow, are shown in Figure 4. Data for three thermocouples are shown: the first and second, from left to right in the nozzle (see Figure 2), and at the base. The third thermocouple in the nozzle (near the throat) failed early on in the testing but, where data was obtained, indicated temperatures similar to the second thermocouple. Wall temperatures are between 300 K and 435 K for the first and base thermocouples, and between 300 K and 350 K for the second. Temperature generally tends to increase at a decreasing rate with time, but steady state is not nearly reached by 60 s of run time. The rate of temperature rise for all thermocouples tends to be greater at greater enthalpy. For the $M_h=7$ data, the first thermocouple indicates a temperature drop 5 s - 15 s into the run that is attributed to the arrival of small amounts of liquid water, flowing on the surface of the nozzle from the heater (see section below "Water Condensation in the Heater"). After two runs at $M_h=7$, some oxidation was noticed near the nozzle throat and no additional runs were performed at this condition. For cases with coflow, the coflow is switched on 5 s - 10 s into the run and ends shortly before the end of the run. Coflow does not significantly affect the first and second thermocouple temperatures. The thermocouple at the base indicates a temperature drop immediately after the coflow is switched on, and thereafter it rises more slowly; coflow reduces the base temperature by 25 K - 50 K.

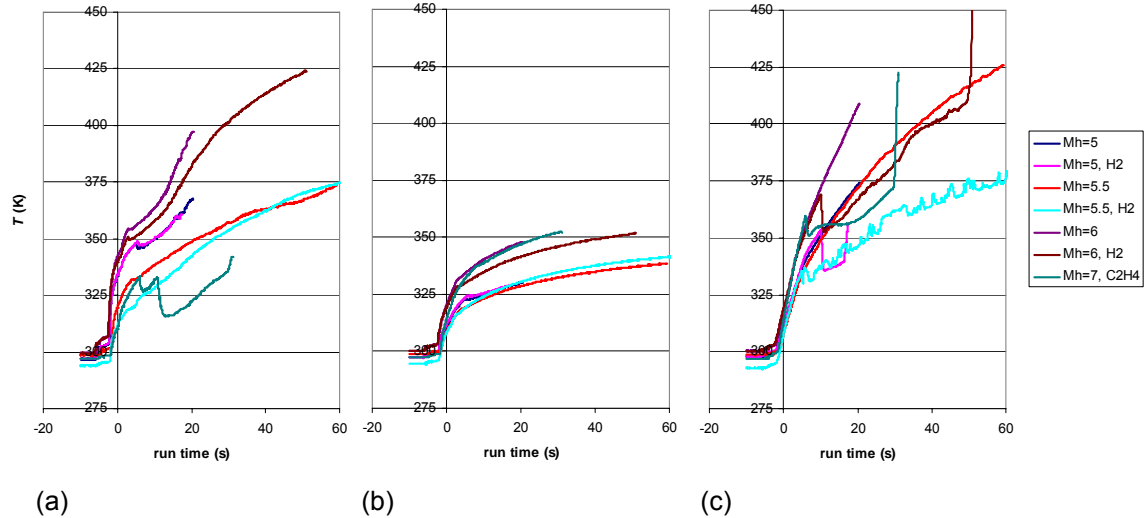


Figure 4. Nozzle wall temperatures: (a) first, (b) second, (c) base thermocouple.

WATER CONDENSATION IN THE HEATER



Figure 5. Condensation water discharge from facility prior to installation of extraction flange.

During early phases of the testing, liquid water was observed in video images, such as Figure 5, discharging from the nozzle exit during facility operation. Water was observed for all test points ($M_h=5, 6, \text{ and } 7$) with an $M=2$ nozzle installed, being greater at the higher enthalpy. This water discharge was unacceptable from the standpoint of the experiment as it interferes with the CARS-IRS optical system, and it would enter into the flow at the mixing layer between the vitiated air center jet and the fuel coflow, altering this most important region of the flow. Two hypotheses were advanced for the source of this water: leakage from the heater cooling circuits and condensation from the combustion products on the relatively cool heater inner liner. No water was discharged when the facility was operated with cooling flow and with flow of gases (air), but with no combustion. Nor was water leakage observed when the nozzle was removed and the heater inspected, with cooling flow on. For normal rates of cooling flow at the $M_h=6$ test point, thermocouples installed in the heater liner indicated temperatures at the end of a 30 s facility run of 364 K at 0.94 m from the end of the heater and 315 K at 0.23 m from the end. These temperatures increased to 440 K and 349 K, respectively, when the cooling water was reduced to approximately 1/5th of the normal rate: however, the temperature was rising steadily during the run and was not near the steady state by the end. At this test point the temperature at which the water vapor in the combustion products becomes saturated is approximately 375 K, above the temperature of the liner, at least at the downstream end. Thus, it was tentatively

concluded that the source of the water is condensation, and further, that the problem could not be eliminated by reducing the cooling flow to the heater.

A water extraction flange was installed between the nozzle and the heater, which contains two 6 mm drain holes at the bottom to collect and drain condensate from the heater during a facility test, before it enters the nozzle region. Tubes ran from these holes to a bucket where liquid is collected: typical rate of collection is 115 ml – 150 ml per 30 second test. In addition to the liquid water, some gas is discharged from the drain holes, but the amount is considered small in comparison to the total rate of flow in the heater. After installation of these drain holes, video images similar to Figure 5 showed only a small amount of liquid water flow, occurring during the early part of the test on the nozzle surface upstream of the throat. No liquid water flow could be seen on the surface downstream of the throat, nor could any discharge into the jet flow be seen. This configuration was used for all subsequent tests. A chemical analysis of the discharge lent further weight to the hypothesis that the discharge was water that had condensed on the relatively cool inner liner of the heater, not cooling water, since certain dissolved chemical constituents expected in the cooling tower water were not present in the discharge.

FLAME VISUALIZATIONS

LABORATORY FLAMES

Flame imaging results for the laboratory flames have been presented previously for a wide range of flames.²⁰ More recent images are presented in Figure 6 and Figure 7, to provide a direct comparison between the flames in the laboratory and at the large scale.

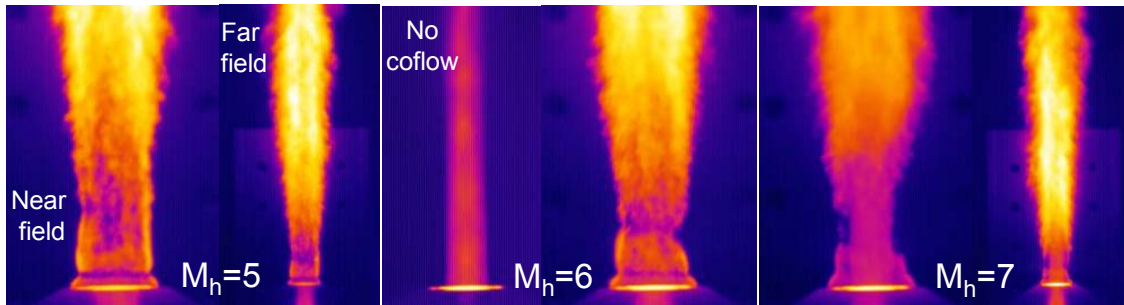


Figure 6. Laboratory flames imaged in the IR with coflow of H₂ at $\phi=1$: near field and far field views at $M_h=5, 7$; near field closeup with and without coflow at $M_h=6$.

Figure 6 shows IR images with H₂ coflow and M_h equal to 5, 6, and 7 (from left to right). At M_h equal to 5 and 7, close up images near the nozzle exit and images of the complete flame are shown. At M_h equal to 6, an image without coflow combustion and a close up image near the nozzle exit are shown. Flow is from bottom to top. There is a very pronounced difference between the images with coflow combustion and without. With H₂ coflow, an *edge attached flame* is formed, attached to the nozzle exit and following the interface between the coflow and the surrounding ambient air. There is no visual evidence in the IR or visible light images with H₂ coflow (e.g., Figure 7a) of combustion within the region of flow recirculation at the base. Turbulent flow structures appear to be sharply resolved at the outer boundary of the flame. The flow velocity of the center jet is approximately 1000 m/s (at $M_h = 5.5$). So, in the exposure time of the camera, structures moving at this speed would be expected to move approximately 12 mm and would therefore result in a blurred image. These edge structures must therefore move at much lower speed than the center jet. As the enthalpy Mach number is increased, the flame appears to weaken near the nozzle exit and begin to detach from the nozzle. This trend must be

due to the increase in velocity of the centerjet which increases the strain rate at the coflow-ambient air interface, tending to extinguish the flame there. Without coflow, the centerjet is clearly visible, although structures at its edge are blurred due to the speed of the jet and the exposure time of the camera.

Figure 7 shows IR and visible light images with (a) coflow of H_2 at $\phi=1$, $M_h=6$, and (b) coflow of C_2H_4 at $\phi=1$, $M_h=7$. With H_2 coflow, the visible light image shows the flame to be pale bluish-white color due to emission from the OH radical; the long exposure time of the camera results in a smooth appearance of the flame. With C_2H_4 coflow there is very distinctive blue flame due to emission from CH radicals, indicating some chemical reaction does take place; however, the IR emission as compared to the jet with no coflow shows very little additional IR emission, indicating little heat release and therefore incomplete reaction. In comparison with the H_2 flame, the C_2H_4 is narrower, except near the downstream end.

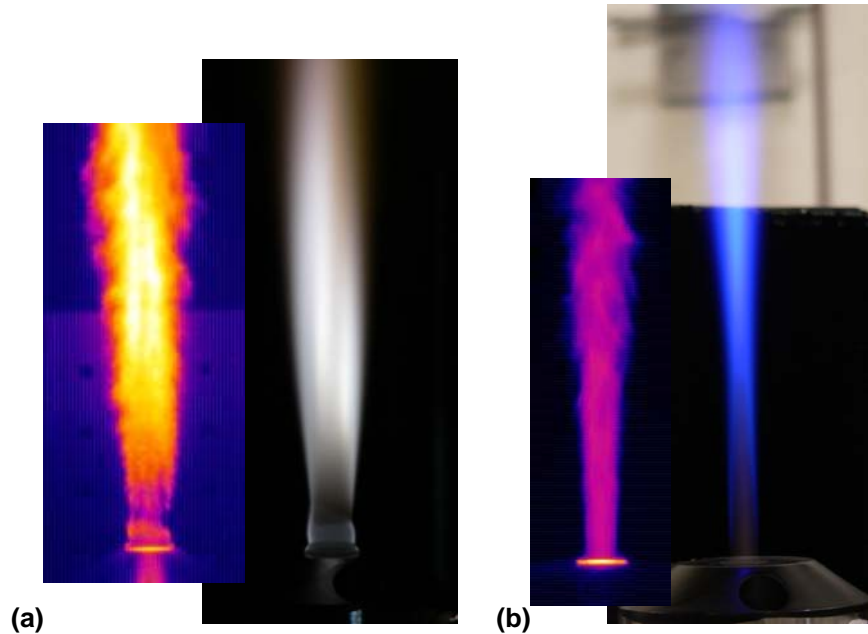


Figure 7. Laboratory flames imaged in the visible and IR: (a) coflow of H_2 at $\phi=1$, $M_h=6$; (b) coflow of C_2H_4 at $\phi=1$, $M_h=7$.

LARGE SCALE FLAMES

Flame imaging results for the large scale flows are shown in Figure 8 - Figure 13: the centerjet enthalpy, coflow fuel type, coflow equivalence ratio, and flame state for these cases are summarized in Table 2. A more detailed discussion of these figures follows.

Figure 8 shows a sequence of images from a single run with $M_h=5.5$ and a stoichiometric H_2 coflow ($\phi_{H_2}=1$). The first image shows the center jet during facility startup, just before the facility heater has achieved final flow rates, and before the coflow is started: a diamond shock pattern, typical of a supersonic jet with exit pressure below atmospheric, may be observed. The main purpose of this image is to show that the IR technique shows clearly the presence of the diamond shock pattern, if such a pattern exists. The second image (B.a) was taken shortly after final flow rates have been established, but before the coflow. A smooth shock-free jet flow is visible, with some larger turbulent flow structures towards the downstream end of the field of view. The third image (B.b) is after the coflow has been established and shows an attached flame at the coflow-atmospheric air interface, very similar to the flames observed for the laboratory burner in Figure 6. As with the laboratory burner, turbulent flow structures are clearly visible at the outer boundary of the flame, although many of these are smaller relative to the nozzle diameter than in the laboratory. This may be because either the smallest scales of

turbulence are relatively smaller at higher Reynolds number or the smallest structures in the smaller flow are more blurred by the effects of motion and the finite exposure time of the camera.

Case	M_h	ϕ_{H_2}	$\phi_{C_2H_4}$	flame state
A	5	1.1	0	none
B.a	5.5	0	0	none
B.b	5.5	1	0	attached
C.a	5.5	0.55	0	detached
C.b		0.55	0.43	further detach
D	6	1.31	0	attached
E.a	6	0.7	0	attached
E.b		0.7	0.53	attached
F.a	6	0.49	0	detached
F.b		0.49	0.47	further detach
G.a	6	0.64	0	attached
G.b		0.64	0.49	attached
G.c		<0.4	0.49	detached
H	6	0	0.9	none
I	7	0	1	detached

Table 2. Large scale facility test cases, nominal operating conditions, and corresponding flame states.



Figure 8. IR images of large scale flame during facility startup, Cases B.a ($M_h=5.5$), and B.b ($M_h=5.5$, H_2 coflow at $\phi=1$).

Figure 9 shows visible and IR light images for two cases with $M_h=6$: the left-hand images (E.a) have H_2 coflow and the right (E.b) have a mixture of H_2 (at the same flow rate) and C_2H_4 . In both cases, attached flames are observed. The second case is blue in color due to emission from CH radicals and, although not evident in the images, is much brighter in the visible light (the camera exposure adjusted automatically). Turbulent structures at the edge of the flame are smoothed out in these images due to the long integration time of this camera. The corresponding IR light images are shown directly above the visible at approximately the same scale. The images show essentially the same features except that turbulent structures are resolved. Note that differences in the appearance of beams and optical components between the visible and IR images are due to differences in the viewing angle (visible views vertically down and IR views horizontally).

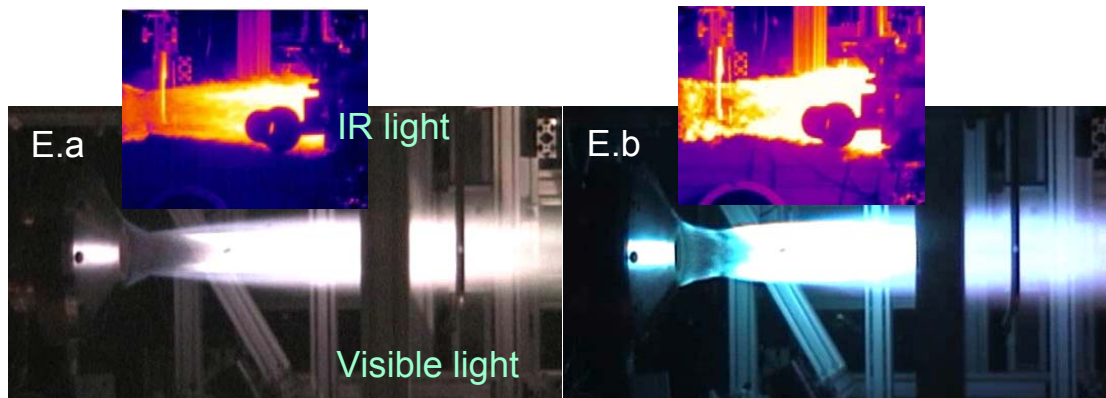


Figure 9. Visible and IR light images of Cases E.a and E.b, $M_f=6$ and H_2 or mixed H_2 - C_2H_4 coflow showing attached flames.

Figure 10 shows several visible and IR images for two cases with $M_f=5.5$: the left-hand images (C.a) have H_2 coflow and the right (C.b) have a mixture of H_2 (at the same rate) and C_2H_4 . In both cases the flames are detached from the nozzle exit, being detached further downstream in the second case. Sequences of images in the IR (C.a) and in the visible (C.b) show that in both cases the flame is unsteady at large scale, moving up and downstream over a significant distance at relatively low frequency (approximately 10 Hz – 100 Hz). (The frequency is known to be this low since some of this motion is resolved by the visible camera.) Figure 11 shows IR images for two cases with $M_f=6.0$: the left-hand image (F.a) has H_2 coflow and the right (F.b) has a mixture of H_2 (at the same rate) and C_2H_4 . Figure 12 shows IR images for three cases with $M_f=6.0$: the first image (G.a) has H_2 coflow, the second (G.b) has a mixture of H_2 (at the same rate) and C_2H_4 , and the third (G.c) is in the process of reducing H_2 . The first two cases are similar to the cases in Figure 9, and show attached flames; the third image shows the flame in the process of detachment from the nozzle, and may be compared to the right hand images in Figure 6 which show a similar process in the laboratory burner. In summary, inspection of the image sequences, typified by the images shown, indicate a trend toward detachment and downstream movement of the flame as the flow of H_2 is reduced, and as C_2H_4 is added to the H_2 .

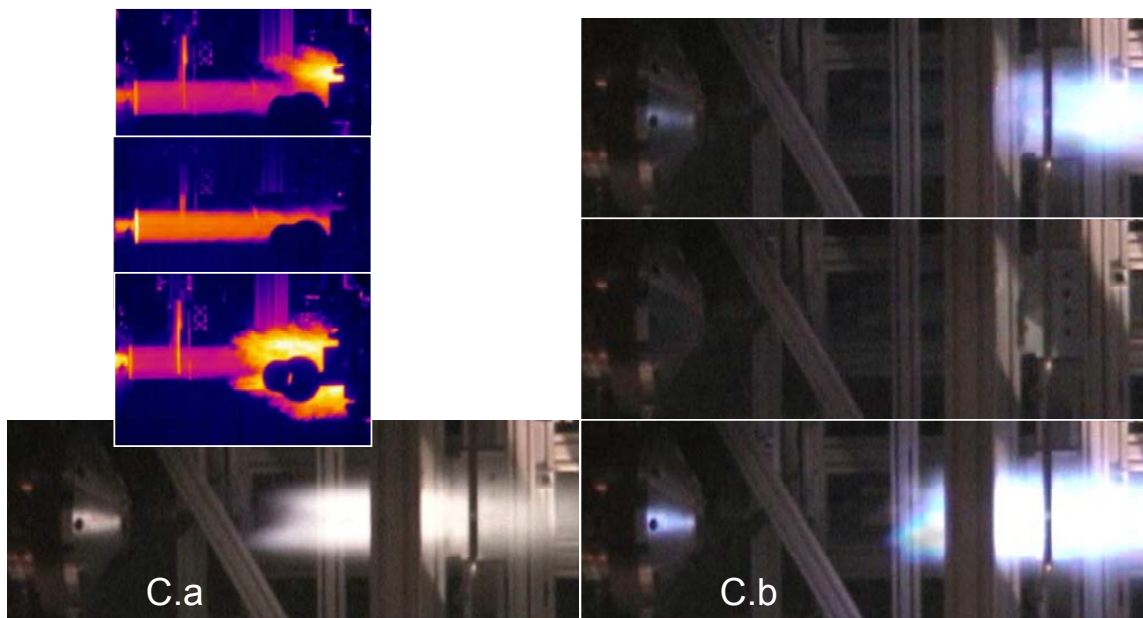


Figure 10. Visible and IR light images of Cases C.a and C.b, $M_f=5.5$ and H_2 or mixed H_2 - C_2H_4 coflow, showing detached, unsteady flames.

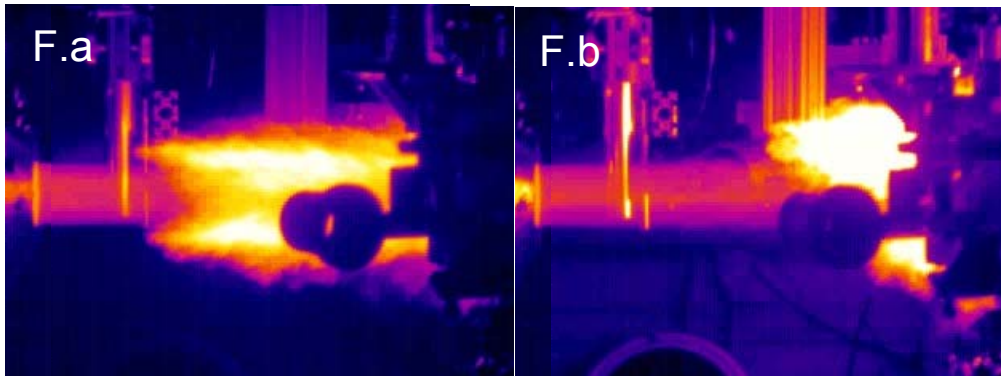


Figure 11. Cases F.a and F.b, $M_f=6$ and H_2 or mixed $H_2-C_2H_4$ coflow, showing detached, unsteady flames.



Figure 12. Cases G.a, G.b, G.c, $M_f=6$ and H_2 or mixed $H_2-C_2H_4$ coflow, showing detachment as H_2 rate is decreased.

No flame was observed at all with $M_f=6$ and pure C_2H_4 coflow (H – see Table 2). Figure 13 shows a single visible image for $M_f=7$ and C_2H_4 coflow (I): a very intense detached flame is observed in this case. This image may be contrasted with Figure 7b, which shows relatively little combustion in the laboratory flame for the same nominal condition.

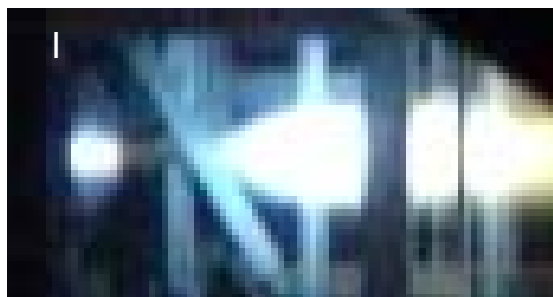


Figure 13. Visible light image for Case I, $M_f=7$ and $H_2-C_2H_4$ coflow, showing intense detached flame.

TEST CASES FOR CARS-IRS STUDIES

Three test cases are identified for study with the CARS-IRS optical system to provide detailed data for CFD model development. These cases represent a sequence of increasing complexity which together allow several models to be calibrated.

The first case is an $M = 1.6$ $M_h = 5.5$ center jet of vitiated air with no coflow and no jet combustion (Figure 8 B.a). Temperature gradients in the mixing layer with the surrounding air are large but composition gradients are not very large. Important turbulence models in this flow are the models for Reynolds shear stress and Reynolds heat flux. The CARS-IRS data set has been acquired and preliminary results are presented in the companion paper.¹⁹

The second case is a $M_h = 5.5$ center jet of vitiated air with H_2 coflow and $\phi_{H_2} = 1$ (Figure 8 B.b). This case has an attached flame. In addition to the turbulence models above, the model for Reynolds mass flux is important. Also, the flow is complicated by heat release in the shear layer that should provide a more rigorous test of the heat flux model. CARS-IRS data has been acquired for this case, but the data set is not complete.

The third case is a $M_h = 5.5$ center jet of vitiated air with a coflow mixture of H_2 and C_2H_4 (Figure 9 E.b). This case also has an attached flame. It is similar to the previous case but has a more complicated chemistry. This case is of interest because of the importance of hydrocarbon fuels in scramjets.

Prior to the flame visualization studies, it was believed that a detached flame would be a suitable test case for detailed study with CARS-IRS since it would be sensitive to chemistry and turbulence chemistry interaction models. Thus, it would fit into the logical progression of increasing complexity. However, the detached flames are unsteady with time scales much longer than the characteristic turbulence fluctuation time scale of the mixing layer. It is not possible to separate the fluctuations in measured flow properties due to this unsteadiness from fluctuations due to turbulence with available techniques, so it is not possible to measure the statistical properties of the turbulence fluctuations in this flow. Also, this flow would have to be computed with a time-accurate method, so would be more computationally intensive. Finally, these unsteady flames are accompanied by significant (acoustic) noise which poses a structural-vibration problem for the optical systems.

The measured conditions for the CARS-IRS tests accomplished in the DCSCF at this time follows. The average and the standard deviation of facility flow rates (statistics formed including variation within runs and from run to run) are for air flow, O_2 flow, and H_2 flow respectively: 0.920 ± 0.012 kg/s, 0.155 ± 0.005 kg/s, and 0.0147 ± 0.0004 kg/s. The total pressure measured in the facility combustion chamber is $p_t = 414 \pm 27$ kPa. For the second case the H_2 coflow is 0.032 ± 0.004 kg/s. (Uncertainties are given for the 95% probability limits.)

SUMMARY AND CONCLUSIONS

Experiments are described to provide data for development and validation of computational models of turbulent mixing and combustion in scramjet engines. A laboratory scale burner was developed which provides a 10 mm diameter supersonic center jet of combustion products, containing either excess H_2 or excess O_2 ; and, an unheated coflow of air or fuel (H_2 or C_2H_4), respectively. Both cases result in a supersonic flame. This burner was used to test newly developed CARS-IRS optical techniques for flow measurement, and to evaluate flames for more detailed study. A nozzle was developed and integrated with NASA Langley's Direct Connect Supersonic Combustion Test Facility to create a large scale flow similar to the laboratory flow, but scaled by $\times 6.35$. The turbulent flow structures of this larger flow could be better resolved by the optical instrumentation. The center jet in these experiments consisted of combustion products of H_2 in air and O_2 , with O_2 content the same as standard air, and the coflow was of H_2 , or C_2H_4 , or a mixture of both. Facility data and visualization of various flames in this facility, using infrared and visible light cameras, are presented. Test cases for more detailed examination using CARS-IRS were selected based on this visualization. These cases, in order of increasing complexity, are: a case with no coflow and no jet combustion; a case with H_2 coflow and flame attached to the nozzle exit; and a case with an H_2 and C_2H_4 mixture and attached flame. In certain cases, detached flames were observed, but these were unsteady and probably too complex to be useful for the current computational model developments.

ACKNOWLEDGMENTS

The authors acknowledge Barry Lawhorne, and his team at NASA Langley's DCSCFTF, and Lloyd Wilson in the combustion laboratory for their help with these experiments.

REFERENCES

- ¹ Baurle, R.A., "Modeling of High Speed Reacting Flows: Established Practices and Future Challenges," AIAA 2004-267, 42nd Aerospace Sciences Meeting and Exhibit, Reno, NV, 5-8 Jan, 2004.
- ² Cutler, A.D., Danehy, P.M., Springer, R.R., O'Byrne, S., Capriotti, D.P., DeLoach, R., "Coherent Anti-Stokes Raman Spectroscopic Thermometry in a Supersonic Combustor," *AIAA J.*, Vol. 41, No. 12, Dec. 2003.
- ³ Lucht, R.P., "Three-laser coherent anti-Stokes Raman scattering measurements of two species," *Optics Letters*, Vol. 12, No. 2, February 1987, pp. 78-80.
- ⁴ Hancock, R.D., Schauer, F.R., Lucht, R.P. and Farrow, R.L., "Dual-pump coherent anti-Stokes Raman scattering measurements of nitrogen and oxygen in a laminar jet diffusion flame," *Applied Optics*, Vol. 36, No. 15, 1997.
- ⁵ O'Byrne, S., Danehy, P.M., Cutler, A.D., "Dual-Pump CARS Thermometry and Species Concentration Measurements in a Supersonic Combustor, AIAA Paper 2004-0710, 42nd Aerospace Sciences Meeting, Reno, NV, Jan. 5-8, 2004.
- ⁶ Tedder, S. A., O'Byrne, S., Danehy, P. M., Cutler, A. D., "CARS Temperature and Species Concentration Measurements in a Supersonic Combustor with Normal Injection," AIAA Paper 2005-0616, 43rd AIAA Aerospace Sciences Meeting, Reno, NV, Jan 10-13, 2005.
- ⁷ Goyne, C.P., McDaniel, J.C., Krauss, R.H., Day, S.W., "Velocity measurement in a dual-mode supersonic combustor using particle image velocimetry," AIAA Paper 2001-1761, AIAA/NAL-NASDA-ISAS International Space Planes and Hypersonic Systems and Technologies Conference, 10th, Kyoto, Japan, Apr. 24-27, 2001.
- ⁸ Bresson, A., Bouchardy, P., Magre, P., Grisch, F., "OH/acetone PLIF and CARS thermometry in a supersonic reactive layer," AIAA Paper 2001-1759, AIAA/NAL-NASDA-ISAS International Space Planes and Hypersonic Systems and Technologies Conference, 10th, Kyoto, Japan, Apr. 24-27, 2001.
- ⁹ Drummond, J.P., Danehy, P.M., Bivolaru, D., Gaffney, R.L., Parker, P., Chelliah, H.K., Cutler, A.D., Givi, P., Hassan, H.A., "Predicting the Effects of Test Media in Ground-Based Propulsion Testing," 2006 Annual ITEA Technology Review, Cambridge, MA, August 7-10, 2006.
- ¹⁰ Drummond, J.P., Danehy, P.M., Bivolaru, D., Gaffney, R.L., Tedder, S.A., Cutler, A.D., "Modeling Combustion in Supersonic Flows," Proceedings of 3rd International Symposium on Non-Equilibrium Processes, Plasma, Combustion, and Atmospheric Phenomena (NEPCAP 2007), Sochi, Russia, June 25-29, 2007.
- ¹¹ Drummond, J.P., Danehy, P.M., Bivolaru, D., Gaffney, R.L., Tedder, S.A., Cutler, A.D., "Supersonic combustion research at NASA," 2007 Fall Technical Meeting, Eastern States Section of the Combustion Institute, University of Virginia, Oct. 21-24, 2007.
- ¹² Bivolaru, D., Danehy, P.M., Lee, J.W., Gaffney, R.L., Cutler, A.D., "Single-pulse, Multi-point Multi-component Interferometric Rayleigh Scattering Velocimeter," AIAA-2006-836, 44th AIAA Aerospace Sciences Meeting, Reno, NV, 9-12 Jan., 2006.
- ¹³ Tedder, S., Bivolaru, D., Danehy, P. M., Weikl, M.C., Beyrau, F., Seeger, T., Cutler, A. D., "Characterization of a Combined CARS and Interferometric Rayleigh Scattering System and Demonstration in a Mach 1.6 Combustion-Heated Jet," AIAA-2007-0871, 45th AIAA Aerospace Sciences Meeting and Exhibit, Reno, NV, Jan. 8-11, 2007.
- ¹⁴ Bivolaru, D., Grinstead, K. D., Tedder S., Lee, J. W., Danehy, P.M., Cutler A. D., "Simultaneous Temperature, Concentration, and Velocity Measurements for Combustion Using CARS and Rayleigh Scattering," AIAA AMT-GT Technology Conference, San Francisco, June, 2007.

- ¹⁵ Bivolaru, D., Danehy, P.M., Gaffney, R.L., Jr., Cutler, A.D., "Direct-View Multi-Point Two-Component Interferometric Rayleigh Scattering System," AIAA 2008-236, 46th Aerospace Sciences Meeting, Reno, NV, Jan 7-10, 2008.
- ¹⁶ Antcliff, R. R., Jarrett, O., Jr., Chitsomboon, T., Cutler, A. D., "CARS Measurements of Temperature and Species Number Density in Supersonic Combusting Flow," AIAA-88-4662, AIAA/NASA/AFWAL Conference on Sensors and Measurement Techniques for Aeronautical Applications, Sep. 7-9, 1988.
- ¹⁷ Gaffney, R.L., Jr., Cutler, A.D., "CFD Modeling Needs and What Makes a Good Supersonic Combustion Experiment," JANNAF Meeting, June 2005.
- ¹⁸ Guy, R.W., Rogers, R.C., Puster, R.L., Rock, K.E., Diskin, G.L., "The NASA Langley Scramjet Test Complex," AIAA-96-3243, 32nd AIAA/ASME/SAE/ASEE Joint Propulsion Conference and Exhibit, Lake Buena Vista, Florida, July 1-3, 1996.
- ¹⁹ Danehy, P.M., Magnotti, G., Bivolaru, D., Tedder, S., Cutler, A.D., "Simultaneous Temperature, Composition, and Velocity Measurements in a Large-scale, Supersonic, Heated Jet," 55th JANNAF Propulsion Meeting, Boston, MA, May 12-16, 2008.
- ²⁰ Cutler, A.D., Magnotti, G., Baurle, R., Bivolaru, D., Tedder, S., Danehy, P.M., Weikl, M.C., Beyrau, F., and Seeger, T., "Development of Supersonic Combustion Experiments for CFD Modeling," AIAA-2007-0978, 45th AIAA Aerospace Sciences Meeting and Exhibit, Reno, NV, Jan. 8-11, 2007.